Theoretical and Experimental Research on Moisture Content and Wood Property Indexes Based on Nondestructive Testing

Liting Cheng,[a,f] Jian Dai,[b,f,]* Zhiguo Yang,[c] Wei Qian,[b,f,]* Wei Wang,[b] Lihong Chang,[d] Xin Li,[e] and Ziyi Wang [a]

A set of reformulated theoretical formulas was developed to measure the relationships between moisture content (MC) and stress wave propagation velocity, dynamic modulus of elasticity (E_d), and modulus of stress-resistograph of the wood. The theory of wood science, elastic mechanics, wave science, and stress wave propagation were used as the theoretical basis. Using larch as the material, both stress wave and micro-drilling resistance technologies were used to study the timber property changes under different moisture contents. The results showed that when the MC of wood did not reach the fiber saturation point (FSP), the wood property decreased sharply with increased MC. However, the study also found that when the MC of wood was higher than the FSP, the wood property decreased with increased MC. In addition, the experimental results showed that the variation trend calculated by the new set of theoretical formulas was consistent with the numerical variation trend measured by the experiment, and the coupling effect of stress wave and micro-drilling resistance was high. This set of theoretical formulas can provide a reference for the research on nondestructive testing and performance evaluation of ancient building timber.

Keywords: Nondestructive testing; Larch; Moisture content; Stress wave; Micro-drilling resistance; Modulus of elasticity; Modulus of stress-resistograph

*Contact information: a: College of Architecture and Civil Engineering, Beijing University of Technology, Beijing 100124, China; b: College of Architecture and Urban Planning, Beijing University of Technology, Beijing 100124, China; c: College of Petroleum Engineering, China University of Petroleum (Beijing), Beijing 102249, China; d: College of Urban and Rural Development, Beijing University of Agriculture, Beijing 102206, China; e: College of Architecture and Art, North China University of Technology, Beijing 100144; f: Beijing Engineering Technology Research Center for Historic Building Protection, Beijing University of Technology, Beijing 100124, China; *Corresponding author:chenglting@126.com*

INTRODUCTION

Wood is an important building material. It plays an important supporting role in the whole architecture system of ancient wooden buildings (Ni *et al.* 2019). Because wood is an anisotropic material, there are many factors that affect wood properties, including density, ring, texture, sapwood difference, moisture content (MC), and other defects (Liu *et al.* 2014). Wood is also susceptible to moisture (Slavik *et al.* 2019). The MC affects the strength, rigidity, and volume stability of the wood within a certain range (Gao *et al.* 2014).

Accurately testing the properties of timber plays a vital role in the safety monitoring and maintenance of ancient building wood members. The commonly used nondestructive testing (NDT) technologies for wood properties include the longitudinal stress wave technology and the micro-drilling resistance testing technology (Zhang *et al.* 2011). The longitudinal stress wave technology estimates the E_d and predicts mechanical strength and properties of wood (Guan *et al.* 2013b). The micro-drilling resistance detection technology detects material changes in wood (Li *et al.* 2016). The combined use of the two technologies can better detect wood properties (Zhu *et al.* 2011).

However, wood MC can influence the accuracy of the two above technologies (Liao *et al.* 2012). The stress wave propagation velocity is a vital detection index in the stress wave technology. The MC has a significant effect on stress wave propagation velocity (Zhu 2012), and the acoustic propagation velocity is negatively correlated with MC within a certain range (Si and Lu 2007; Liu and Gao 2014; Montero *et al.* 2015; Peng *et al.* 2016). The E_d estimated from the stress wave propagation velocity and density also decreases to various degrees with the increase of MC (Moreno-Chan *et al.* 2011; Chang 2017). The degree of decrease is related to the influence of MC on the direction (Chen *et al.* 2012; Wei *et al.* 2019), path of stress wave propagation (Guan *et al.* 2013a), and the temperature (Wang *et al.* 2008, 2009; Gao *et al.* 2009, 2010) in wood. The influences of MC on stress waves propagation velocity and on the E_d are considerably different (Nocetti *et al.* 2015; Llana *et al.* 2018). The difference between E_d and the static modulus of elasticity (MOE) tends to be constant when MC is above FSP (Wang 2008).

The micro-drilling resistance values (including the rotational resistance value of the drilling needle (f_{drill}) and the resistance value of the feeding needle (f_{feed}) are two important detection indexes in the micro-drilling resistance detection technology. The MC affects the size of the resistance. Within a certain range, the resistance may first increase and then decrease with the increase of MC (Sun 2012). Much research has been conducted to evaluate the relationship between MC and wood property detection indexes. The examples include using a ultrasound tester (Gonçalves and Leme 2008; Gonçalves *et al.* 2018), a stress wave tester (Si and Lu 2007), micro-drilling resistance instrument (Sun 2012), or the combined use of the last two in the studies on different tree species (Liao *et al.* 2012), different degrees of decay (Li 2015), and different profiles (Brashaw *et al.* 2004; Carter *et al.* 2005).

This study investigated the in-depth relationship between MC and wood mass testing indicators. This study was developed based on a) the research results of elasticity theory (Yu *et al.* 2014), wave theory (Yang and Wang 2005), and stress wave longitudinal propagation theory (Liu 2014; Dackermann *et al.* 2016), combining the theory of wood and wave propagation; b) the testing technology of stress wave and micro-drilling resistance; and c) the key factors that affect wood properties. In this study, the representative larch specimens were selected as the research material, and the experimental data and the calculated value of the theoretical formula were verified. The results show that the two values and trends are consistent. Thus, this study also developed a set of reformulated theoretical formulas for the relationship between MC and stress wave propagation velocity, E_d, and modulus of stress-resistograph (including the modulus of stress-resistograph of the drilling needle (F_{drill}) and the modulus of stress-resistograph of the feeding needle (F_{feed}). This set of reformulated theoretical formulas provides a reference for timber property detection and preventive protection research of ancient wood architectural members to conduct the nondestructive testing, monitoring, surveying, and repairing of ancient timber structures.

Theory of MC and wood property indexes based on NDT

Dry wood is mainly composed of wood fiber structures. When the MC increases, water molecules preferentially entered the wood fiber structure in the state of combined water. This is the hydrophilic and self-imbibition effect of the wood fiber. When the fiber structure is full of water molecules, the wood FSP is reached. Then, the water molecules continuously fill in the structural gaps between the wood fibers and exist in the state of free water (Fig. 1) (The Kingdom of Wood 2018).

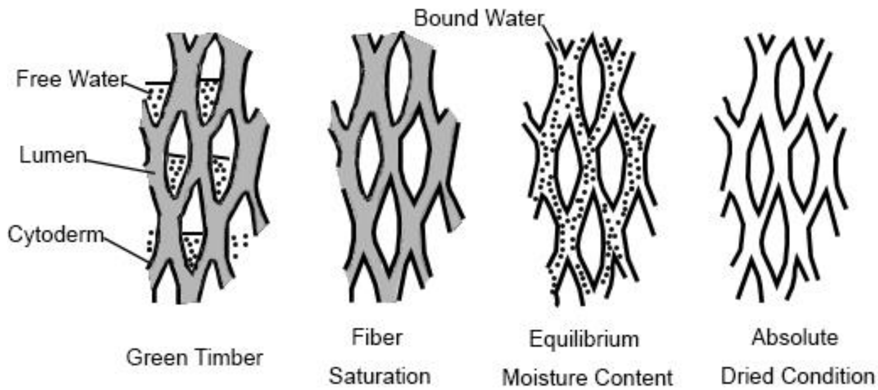

Fig. 1. The state of existence of water in the wood

When the medium in the wood is a continuum, the parameters, such as the density and E_d, of the medium are continuous. The FSP is approximately 30% accordingly. Considering the swelling of the wood after it has absorbed water, the volume of the wood after water absorption is shown in Eq. 1,

$$V = (1 + KW)\, V_0 \tag{1}$$

where V is the volume after wetting (cm^3), V_0 is the volume of wood when absolutely dry (cm^3), K is the wet expansion coefficient (%), $K = S / W$, S is the full wet expansion rate of wood (%), $S = ((V - V_0) / V_0) \times 100$, and W is the difference value between the test and the MC of the wood at the beginning of the test (when the MC is lower than 30%, W is the difference value between the test and the MC of the wood at the beginning of the test; when the MC is greater than 30%, it is 30 (%).

The calculation formula based on density, $d = m / v$, the density of the wood is shown in Eq. 2,

$$\rho_c = (m_o\,(1 + \omega)) / ((1 + KW)\, V_0) \tag{2}$$

where ρ_c is the density of wood (g/cm^3), m_o is the mass of wood substance (g), ω is the MC (absolute MC) (%), $\omega = ((m - m_o) / m_0) \times 100 = ((m / m_o) - 1) \times 100$, m_a is the mass of water in wood (g), and m is the total mass of wood (g), $m = m_o + m_a$ (the mass of the air is small, and is therefore ignored).

The stress waves used in the field of NDT of wood are mostly shock stress waves generated by hammering (Xu 2011). The propagation of stress waves in wood is influenced by properties, direction, and microstructure of wood. It is also closely related to the physical and mechanical properties of wood. There are three common ways the stress waves propagate inside wood: longitudinal propagation, radial propagation, and lateral propagation. Using stress wave technology, the stress waves enter from two-end faces. This belongs to the uniaxial forward propagation and is a one-dimensional stress wave state. Studies (Bertholf 1965) have tested the validity of the hypothesis. Combined with the calculation formula of the longitudinal wave velocity in the propagation theory of stress waves in anisotropic infinite elastic body (Timoshenko and Doodier 1970; Carino and Sansalone 1991), the wave velocity of the stress wave in the wood is shown in Eq. 3,

$$C_o = \sqrt{\frac{E_o\,(1 - \upsilon)}{\rho_o\,(1 + \upsilon)\,(1 - 2\upsilon)}} \tag{3}$$

where C_o is the stress wave propagation velocity in wood (m/s), E_o is the modulus of elasticity of wood (MPa), and υ is the Poisson's ratio.

According to the hypothetical model proposed by Gao (2012), it is assumed that wood is the macroscopic composition of the mixture. The moisture in the wood is all free when the temperature is above 0 °C. The macroscopic view of the wood is composed of wood substance and water. When the MC is ω, the acoustic wave velocity in the wood is shown in Eq. 4,

$$C = \frac{\sum_{i=1}^{n} f_i C_i \sqrt{\rho_i}}{\sqrt{\rho_c}} \tag{4}$$

where C is the sound wave propagation velocity in wood (m/s), f_i is the content of each mixed component of wood (%), C_i is the speed of sound waves in each mixed component (m/s), ρ_i is the density of each mixed component (kg/m^3), and n is 2.

According to Eq. 4, the stress wave propagation velocity in wood is shown in Eq. 5,

$$C_c = \frac{f_o C_o \sqrt{\rho_o} + f_a C_a \sqrt{\rho_a}}{\sqrt{\rho_c}} \tag{5}$$

where C_c is the stress wave propagation velocity in wood (m/s), C_a is the stress wave propagation velocity in water (m/s), f_o is the content of wood substance (%), $f_o = \frac{m_o}{m} = \frac{1}{1+\omega}$, f_a is the content of water in wood (%), $f_a = 1 - f_o = \frac{\omega}{1+\omega}$, ρ_a is the density of water (g/cm^3), and ρ_o *is* the density of wood substance (g/cm^3).

According to the conversion relationship between f_o, f_a, and ω, the stress wave propagation velocity is shown in Eq. 6:

$$C_c = \frac{C_o \sqrt{\rho_o} + \omega C_a \sqrt{\rho_a}}{(1+\omega)\sqrt{\rho_c}} \tag{6}$$

The E_d of wood after it absorbs water is shown in Eq. 7,

$$E_d = \rho_c C_c^{\,2},\ \omega \leq 30\%;\quad E_d = \rho_o{}' C_c^{\,2},\ \omega > 30\% \tag{7}$$

where E_d is the dynamic modulus of elasticity of wood (MPa), $\rho_o{}'$ is the density of the cell wall and wood substance (g/cm^3), $\rho_o{}' = \frac{m_o + m_a{}'}{V}$, and $m_a{}'$ is the mass of sucking water (g), when the wood reaches the FSP, $m_a{}' = 0.3 m_o$.

According to the modulus of stress-resistograph defined by Zhu Lei *et al.* (2011), combined with Eq. 6 and the rotational resistance value of the drilling needle of the micro-drilling resistance instrument, the modulus of stress-resistograph of the drilling needle (F_{drill}) is shown in Eq. 8,

$$F_{drill} = f_{drill} \times C_c^2 \tag{8}$$

where F_{drill} is the modulus of stress-resistograph of the drilling needle (resi·km^2/m^2), and f_{drill} is the rotational resistance value of the drilling needle (resi).

Combining the Eq. 6 and the resistance value of the feeding needle of the micro-drilling resistance instrument, the modulus of stress-resistograph of the feeding needle (F_{feed}) is shown in Eq. 9,

$$F_{\text{feed}} = f_{\text{feed}} \times C_c^2 \tag{9}$$

where F_{feed} is the modulus of stress-resistograph of the feeding needle (resi·km^2/m^2), and f_{feed} is the resistance value of the feeding needle (resi).

EXPERIMENTAL

Materials

Larch wood (*Larix gmelinii*) was selected and used as the experimental material and was purchased from Eastern Royal Tombs of the Qing Dynasty Wood Factory (Tangshan City, Hebei Province, China). The wood is about 300 to 400 years old. According to the standard on the size and method of acquisition requirements for test specimens GB 1929 (2009), the sample was sawn into specimens with a size of 2 cm × 2 cm × 36 cm. Small test specimens of 2 cm × 2 cm × 2 cm were cut from each large test specimen. The specimens of 2 cm × 2 cm × 30 cm were tested for stress wave and micro-drill resistance at different moisture contents, (Figs. 2 and 3).

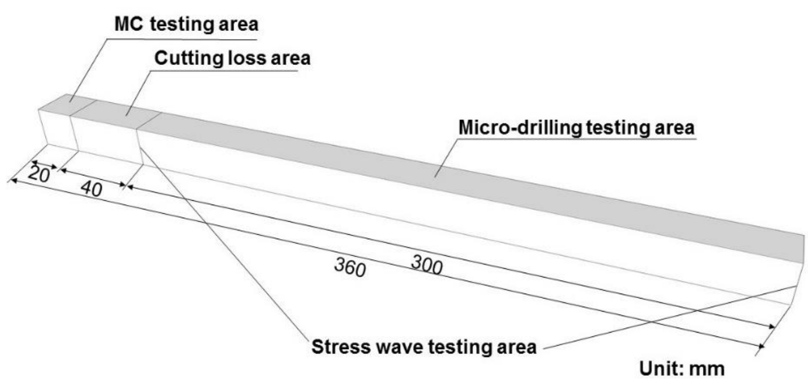

Fig. 2. Experimental specimen partition

Fig. 3. Experimental test specimens

The method of sawing the sample was perpendicular to the direction of rings (Fig. 4). There were 12 specimens. They were from the same log. As one part of the wood was exposed to light and the other part was not during growing, the 12 specimens were divided into two parts, light part and shade part.

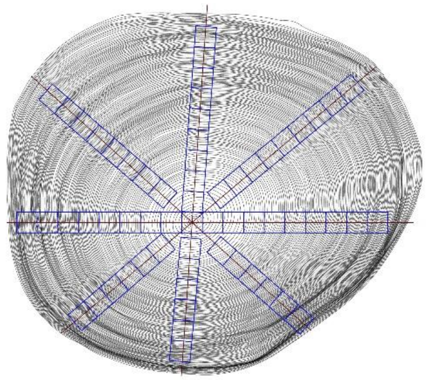

Fig. 4. The method of sawing the sample

Methods

Experiment apparatus

The apparatuses used were a Lichen Technology blast dryer box 101-3BS, Lichen Technology electronic precision balance JA1003 (Shanghai Lichen Electronic Technology Co., Ltd., Shanghai, China), FAKOPP microsecond timber (FAKOPP Enterprise Bt., Ágfalva, Hungary), and an IML-RESI PD500 micro-drill resistance instrument (IML Co., Ltd., Wiesloch, Germany).

Methods and steps

The mass of each small specimen block was measured after drying in the dryer box (Fig. 5). The MC of the test specimens was determined according to GB 1931 (1991) (Fig. 6).

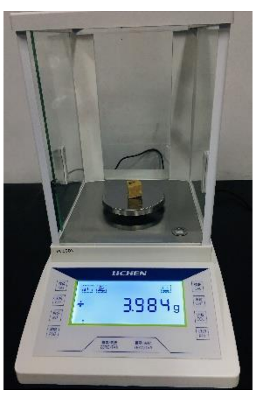

Fig. 5. Small specimen weighing

Fig. 6. Small test specimens drying

At indoor temperature, the test specimens were immersed at intervals of 2 min (0.03 h), 3 min (0.05 h), 5 min (0.08 h), 10 min (0.17 h), 15 min (0.25 h), 30 min (0.5 h), until 96,000 min (1600 h). The mass of the test specimens was measured by an electronic precision balance after each soaking (Fig. 7). And the mass of each test specimen was carried out by mass difference between the mass of the full specimen and the mass of 2cm cubic specimen dried in the oven.

Fig. 7. Specimen weighing

The stress wave was used to measure the propagation time of stress waves in the wood. In this study, the two probes of the instrument were inserted into the two ends of the test specimen and measured along the longitudinal direction of the test specimen. The angle between the two probes and the longitudinal axis of the test specimen was no less than 45°. The distance between the two points was measured (Fig. 8). The propagation time readings of all the taps were measured except the first tap, in which the data was found invalid. The results were then calculated by measuring the average value of three continuous tapping times from the second tap. The propagation velocity of the stress wave in the test specimen was calculated using Eq. 10,

$$C_c = 10^6 \times \frac{L}{T} \tag{10}$$

where L is the distance between the two sensors of the stress wave tester (m), and T is the time recorded between the two sensors of the stress wave tester (μs). The dynamic elastic modulus of wood was calculated using Eq. 11:

$$E_d = \rho_c C_c{}^2 \tag{11}$$

The resistance value of the wood interior material was measured using an IML-RESI PD500 micro-drill resistance instrument. One probe was drilled into the surface of the finished test specimen at a constant speed and perpendicular to the annual ring direction. This is shown in Fig. 9. The data were then entered into the computer to calculate the resistance value. The wave resistance modulus was also calculated, combining the micro-drill resistance values and the stress wave propagation speed (see Eq. 12 and Eq. 13):

$$F_{drill} = f_{drill} C_c{}^2 \tag{12}$$

$$F_{feed} = f_{feed} C_c{}^2 \tag{13}$$

Fig. 8. Determination of stress wave propagation time of specimen

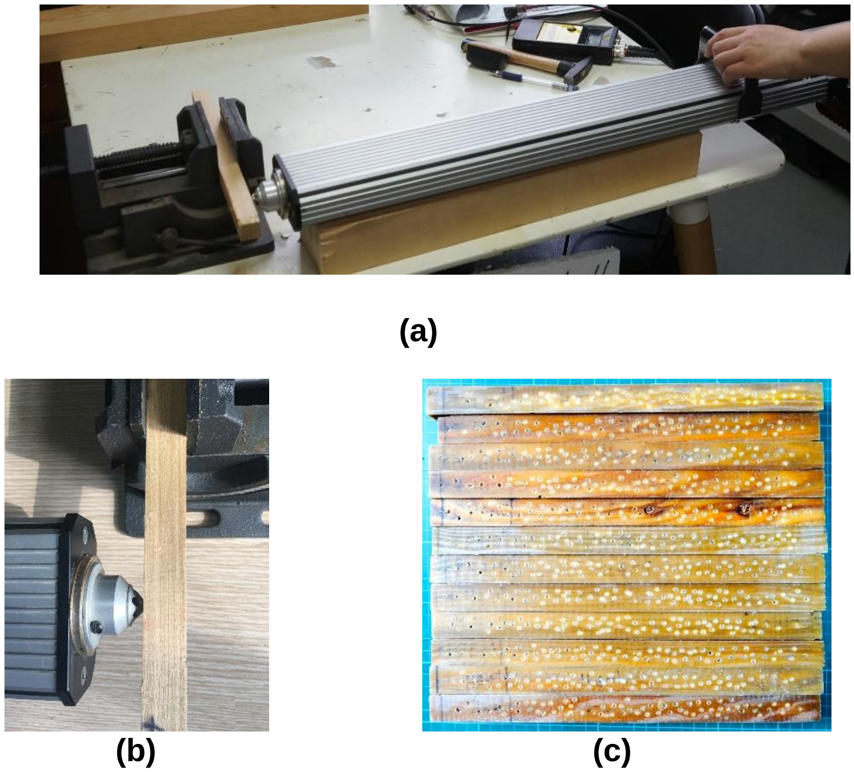

Fig. 9. Determination of the resistance values of the micro-drilling of the test specimens

RESULTS AND DISCUSSION

The selected wood specimens were divided into the shade part and light part. The average data was collected by measuring the shade and light parts to represent the overall timber properties. The MC of wood specimens changed with time (Fig. 10). The trend of wood specimens' density with MC is shown in Fig. 11.

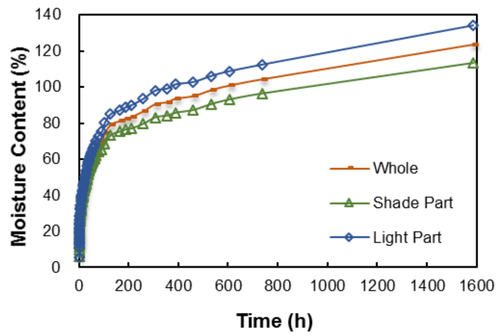

Fig. 10. MC changes with time

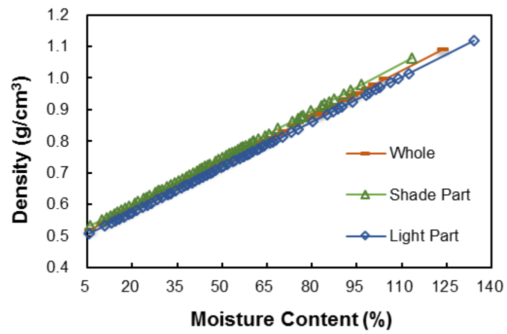

Fig. 11. Density changes with MC

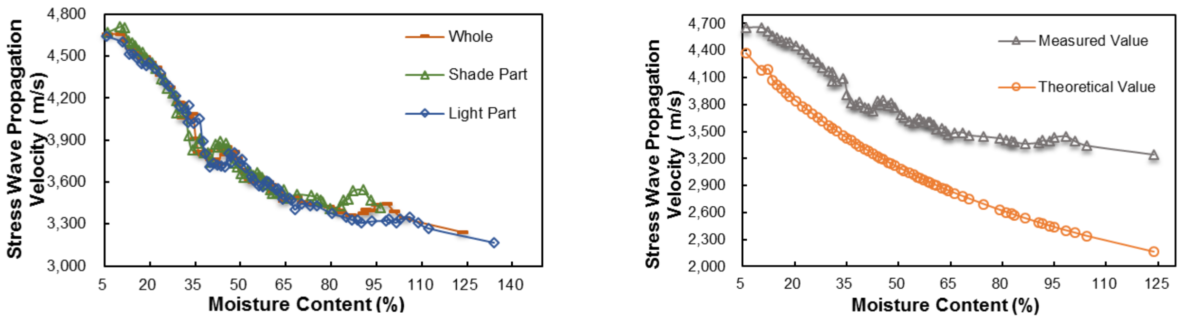

(a) (b)

Fig. 12. (a) Stress wave propagation velocity varies with MC, (b) comparison of the theoretical and measured values

The theoretical calculation values of the stress wave propagation velocity, E_d, and modulus of stress-resistograph of the wood specimens, were calculated to compare with the experimentally measured values (Figs. 12 through 15).

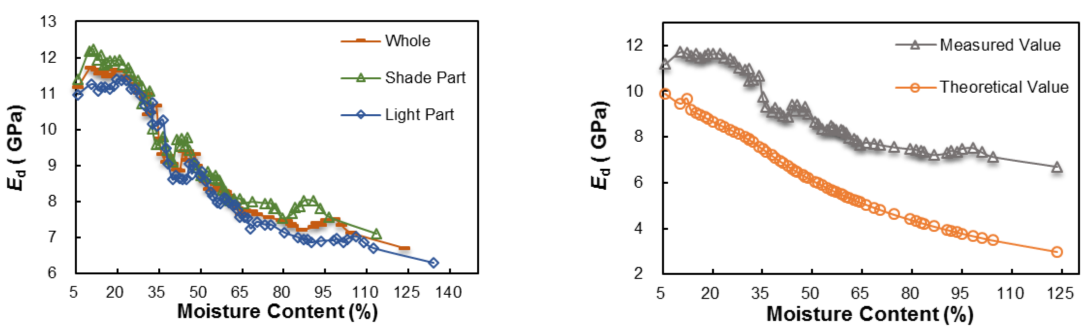

(a) (b)

Fig. 13. (a) E_d varies with MC and (b) comparison of the theoretical and measured values

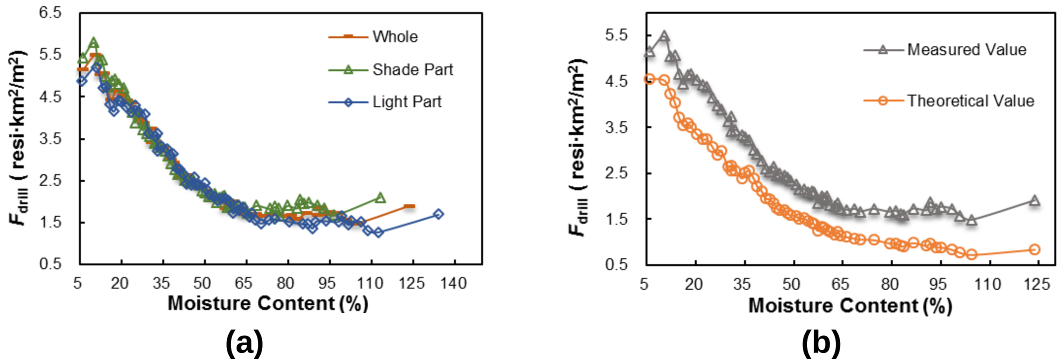

Fig. 14. (a) F_{drill} varies with MC and (b) comparison of the theoretical and measured values

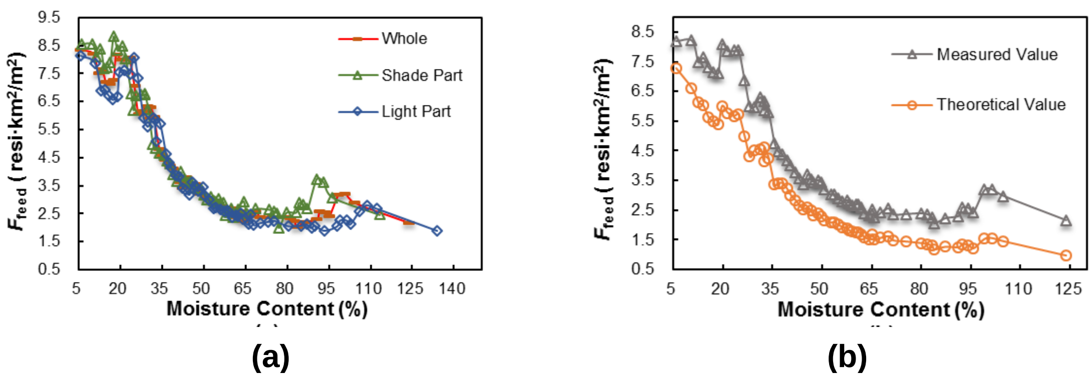

Fig. 15. (a) F_{feed} varies with MC and (b) comparison of the theoretical and measured values

Analysis of wood MC with immersion time

The MC increased with immersion time. When the time reached approximately 100 h, the MC increased to approximately 80%. After that, the increase in MC trend began to gradually slow down. The increase rate in MC during the 0 to 100 h period was 20 times the increase rate during the 100 to 1600 h period. This was because when the wood absorbed moisture, the distance between the microfibrils in the cell wall increased. Thus, the cell wall thickened, and the wood expanded. When the MC exceeded the FSP, the wood did not expand any longer, and the water absorption speed gradually stopped. It was also found that the water absorption capacity of the light part was stronger than that of the shade part. It was because the wood at light part grew faster than the shade part. The wood fiber of the light part was loose; the annual ring gap was large, and the cells were large. Therefore, the water absorption of the light part was stronger and the MC increased faster than the shade part.

Analysis density of wood with MC

Wood density increased with its MC; they were positively correlated with each other. It was found that the density value of the shade part was higher than that of the light part at the same level of the MC. This indicated that the wood fiber of the woody surface was denser in the shade part, compared to the light part.

From Fig. 11, the relationship between density and MC was linear. The linear regression model is: ρ_c = 0.004852 ω + 0.4899. From the linear regression, dividing the slope of the linear regression by the value of density at 12% obtained from the linear regression, one can achieve the adjustment coefficient to 12% MC, and the value was 0.0099. Similar to the value in European standard EN 384 (2004) 0.005, which was obtained from softwoods of Central and North Europe.

Variation of wood stress wave propagation velocity with MC and comparative analysis

The stress wave propagation velocity decreased with the increase of MC. When the MC was greater than 35%, the stress wave propagation velocity decreased gradually. The calculated value of the theoretical formula was lower than the measured value, and the difference value between the two increased with the increase of MC. It was within the range of 290 m/s and 1080 m/s. It was observed that when the MC was lower than the FSP, the wood fiber continuously absorbed water until it was fully saturated. It was also found when the MC was higher than the FSP, the lignocellulosic fiber was already filled with water molecules, and the rate of self-priming slowed down. The wood absorbs moisture in the state of free water, and the stress wave reflects and refracts between the wood fiber and the water molecule; it is affecting the stress wave propagation velocity.

In Fig. 12a the tendency is more or less linear MC from 10% to 30%, and after that, there is a difference, a change between 30% and 40%. The linear regression model of velocity-MC from 10% to 30% is: $C_c = -33.19\ \omega + 4527$. And the slope of the velocity-MC curves is -33.19. Meanwhile, one can obtain the adjustment coefficient (an adjustment coefficient of the velocity by the MC has been defined in terms of a percentage of velocity increase for each percentage point of MC decrease (Montero *et al.* 2015)) as slope/$Vel_{12\%}$ and slope/$Vel_{0\%}$ are both 0.0073. There were similar previous findings (Table 1).

Table 1. Adjustment Coefficient of the Velocity by the MC

MC (%)	Species	Adjustment coefficient	References
11.8	*Pinus sylvestris*	0.0050	Montero *et al.* 2015
0	Japanese cedar lumber	0.00616	Yamasaki *et al.* 2017
12	*Eucalyptus grandis*	0.0066	Gonçalves *et al.* 2018
12	*Corymbia citriodora*	0.0083	
12	*Eucalyptus pellita*	0.0067	
11.6	Radiata pine	0.0056	Llana *et al.* 2018
12.2	*Pinus sylvestris*	0.0053	
12.6	Salzmann pine	0.0093	
11.5	Maritime pine	0.0083	

Variation of E_d with MC and comparative analysis

The E_d decreased with the increase of MC. When the MC reached approximately 80%, the decrease of the E_d gradually slowed down. These results were consistent with the findings from previous studies. According to Wang' study (Wang 2008), below FSP, E_d of Douglas-fir lumber increased continuously as moisture content decreased. Above FSP, E_d remained relatively constant. And the theoretical formula was lower than the measured value. The difference value between the two was 2 to 3 GPa, and the value gradually increased with the increase of MC. This showed that the E_d of wood was affected by the combination of density, stress wave propagation velocity, and percentage of each component.

Variation of modulus of stress-resistograph with MC and comparative analysis

The modulus of stress-resistograph of the drilling needle F_{drill} gradually decreased with the increase of MC. When the MC was greater than 50%, the decreasing trend began to slow down. The theoretical value was lower than the measured value. The difference value was between 0.6 to 1 resi·km^2/m^2.

The modulus of stress-resistograph of the feeding needle F_{feed} gradually decreased with the increase of MC. When the MC was greater than 50%, the decreasing trend began to slow down. When the MC was 20%, there was a jump of the wave resistance modulus. This was a margin of error caused by the uneven distribution of moisture absorbed by the wood. The theoretical value was lower than the measured value. The difference value was 0.7 to 2.2 resi·km^2/m^2.

Reformulated formulas

This study investigated and compared the theoretical value with the actual measurement. It was found that there were reflecting and refracting of the stress wave from the wood fiber to the water, and the two materials influenced each other. It was also noted that the stress wave tester and the micro-drilling resistance instrument had certain margins of error. Thus, to consider all the influencing factors, the older theoretical formula must be revised and modified. According to the book *Wood Science* (Cheng 1985), the bulk swell coefficient K of the larch is 0.588%, the Poisson's ratio υ is 0.42, and the MOE of the larch is 14.1 GPa (Cheng 1985). Setting 12 GPa as the average of the measured values, and combining with C_a = 1450 m/s, ρ_a = 1.0 g/cm^3, and ρ_o = 1.5 g/cm^3 (Cheng 1985), the researchers reformulated the theoretical formulas for the wood materiality detection index through the set of formulas of a) stress wave propagation velocity in Eq. 14, b) E_d in Eq. 15, c) F_{drill} in Eq. 16, and d) F_{feed} in Eq. 17 (Table 2).

Table 2. Reformulated Formulas for Wood Materiality Detection Index

Indicator Name	Reformulated Formulas
Stress wave propagation velocity	$C_c = \dfrac{C_o\sqrt{\rho_o} + \omega C_a\sqrt{\rho_a}}{(1+\omega)\sqrt{\rho_c}} + C(\omega)$ $C(\omega) = 181.4\omega^{0.3811}$, $\omega \le 30\%$; $C(\omega) = 50.93\omega^{0.6346}$, $\omega > 30\%$ （14）
E_d	$E_d = \rho_c C_c^2 + E(\omega)$， $E(\omega) = 0.7868\omega^{0.4178}$, $\omega \le 30\%$; $E_d = \rho_o' C_c^2 + E'(\omega)$， $E'(\omega) = 0.01694\omega + 1.786$, $\omega > 30\%$ （15）
Modulus of stress-resistograph of the drilling needle	$F_{drill} = f_{drill} C_c^2 + F_{drill}(\omega)$ $F_{drill}(\omega) = 0.4975\omega^{0.2409}$, $\omega \le 30\%$; $F_{drill}(\omega) = 3.422\exp(-0.06355\omega) + 0.3174\exp(0.009617\omega)$, $\omega > 30\%$ （16）
Modulus of stress-resistograph of the feeding needle	$F_{feed} = f_{feed} C_c^2 + F_{feed}(\omega)$ $F_{feed}(\omega) = 0.7677\omega^{0.265}$, $\omega \le 30\%$; $F_{feed}(\omega) = 68.62\exp(-0.1415\omega) + 0.5487\exp(0.008117\omega)$, $\omega > 30\%$ （17）

The theoretical calculation formulas were modified before and after the detection data, and the comparison results are shown in Figs. 16 to 19.

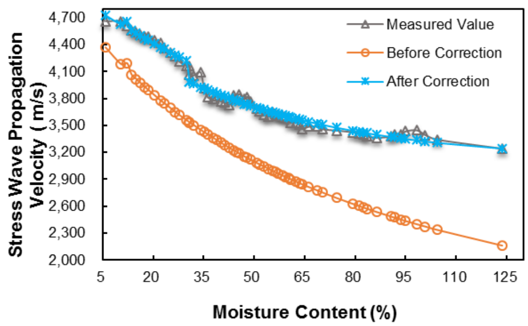

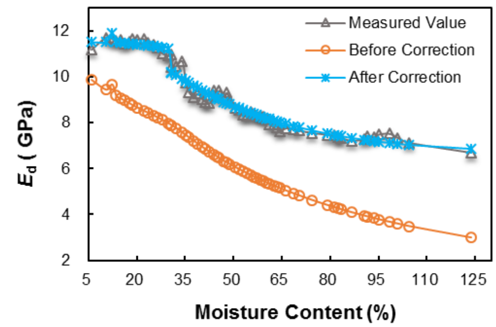

Fig. 16. Comparison of the stress wave propagation velocity

Fig. 17. Comparison of the E_{d}

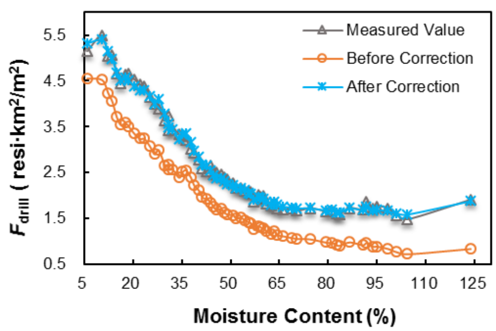

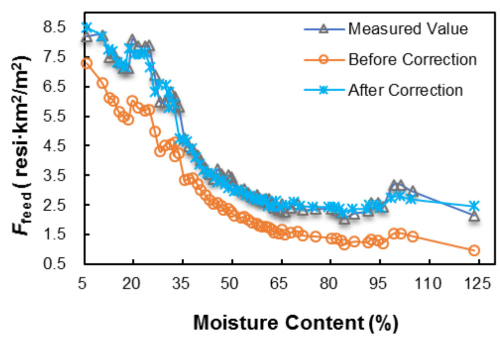

Fig. 18. Comparison of the F_{drill}

Fig. 19. Comparison of the F_{feed}

This study also found that the results calculated from the set of reformulated theoretical formulas were consistent with the measured values of the measured index values, and the combined use of the stress wave and the micro-drilling resistance was more effective in detecting the wood performance indexes. This new set of theoretical formulas provides a theoretical basis for the detection of larch wood, as well as a reference for the detection of other tree species.

CONCLUSIONS

1. The relationships between moisture content (MC) and larch property indexes were established. The theoretical and experimental results showed that when the MC did not reach the fiber saturation point (FSP), the wood properties decreased sharply with increased MC. However, when the MC was higher than the FSP, the trends began to slow down.
2. The larch density value of the shade part was higher than that of the lighted part at the same level of the MC. According to the linear regression model between density and MC, an adjusted coefficient at 12% MC of 0.0099 was determined.
3. According to the model of velocity-MC from MC 10% to 30%, the larch adjusted coefficient of the velocity by the MC was found to be 0.0073.

4. The variations of modulus of stress-resistograph of drilling and feeding exhibit a change with MC after 50% MC and not around the FSP as has been observed for stress waves.
5. The experimental results showed that the combined use of stress wave and micro-drill resistance was more effective than the other effects.
6. This study investigated the relationships between the MC of the larch and stress wave propagation velocity, E_d, modulus of stress-resistograph of the drilling needle, and modulus of stress-resistograph of the feeding needle. It provides a theoretical basis for the construction of the investigation work, safety survey work, maintenance work, and wood material condition determination in the NDT project of ancient building wood structure.

ACKNOWLEDGMENTS

The study was supported by the National Natural Science Foundation of China (51678005).

REFERENCES CITED

Bertholf, L. D. (1965). *Use of Elementary Stress Wave Theory for Prediction of Dynamic Strain in Wood* (Bulletin 291), Washington State University, Pullman, WA, USA.

Brashaw, B., Wang, X., and Ross, R. (2004). "Relationship between stress wave velocities of green and dry veneer," *Forest Products Journal* 54(6), 85-89. DOI: 10.1023/B:CELL.0000025379.34900.df

Carino, N., and Sansalone, M. (1991). "Impact-echo: A new method for inspection construction material," in: *Nondestructive Testing and Evaluation for Manufacturing and Construction: Conference Proceedings*, Dos Reis, Brazil, pp. 209-223. DOI: 10.1016/0963-8695(91)90435-6

Carter, P., Wang, X., Ross, R., and Briggs, D. (2005). "NDE of logs and standing trees using new acoustic tools: Technical application and results," in: *14th International Symposium on Nondestructive Testing of Wood: Conference Proceedings*, Eberswalde, Germany, pp. 161-169.

Chang, L. (2017). *Research on Wooden Components Damages and Material Property Appropriate Technology Test of Buildings Based on Preventive Protection*, Ph.D. Dissertation, Beijing University of Technology, Beijing, China.

Chen, Y., Li, H., Li, D., and Zhang, T. (2012). "Effects on stress wave speed inside wood members in historical building," *China Wood Industry* 26(2), 37-40. DOI: 10.19455/j.mcgy.2012.02.010

Cheng, J. (1985). *Wood Science*, China Forestry Publishing House, Beijing, China.

Dackermann, U., Elsener, R., Li, J., and Crews, K. (2016). "A comparative study of using static and ultrasonic material testing methods to determine the anisotropic material properties of wood," *Construction and Building Materials* 102(2), 963-976. DOI: 10.1016/j.conbuildmat.2015.07.195

Gao, S. (2012). *Effect of Environmental Temperature on Acoustic Mechanical Properties of Standing Trees and Logs*, Ph.D. Dissertation, Northeast Forestry University, Harbin, China.

Gao, S., Wang, L., and Wang, Y. (2009). "A comparative study on the velocities of stress wave propagation in standing *Fraxinus mandshurica* trees in frozen and non-frozen states," *Frontiers of Forestry in China* 4(4), 382-387. DOI: 10.1007/s11461-009-0064-9

Gao, S., Wang, L., and Wang, X. (2014). "The influence of temperature and moisture contents on modulus of elasticity of *Pinus koraicnsis* wood," *Forestry Science and Technology Development* 28(4), 38-42. DOI: 10.13360/j.issn.1000-8101.2014.04.010

Gao, S., Wang, L., Wang, Y., and Xu, H. (2010). "Comparisons of stress wave propagating velocities in frozen state and in normal temperature state standing trees," *Scientia Silvae Sinicae* 46(10), 124-129. DOI: 10.11707/j.1001-7488.20101021

GB 1929 (2009). "Method of sample logs sawing and test specimens selection for physical and mechanical tests of wood," Standardization Administration of China, Beijing, China.

GB 1931 (1991) "Method for determination of the moisture content of wood," Standardization Administration of China, Beijing, China.

Gonçalves, R., and Leme, O. A. (2008). "Influence of moisture content on longitudinal, radial and tangential ultrasonic velocity for two Brazilian wood species," *Wood and Fiber Science* 40(4), 580-586. DOI: 10.1007/s00468-008-0234-7

Gonçalves, R., Mansini-Lorensani, R. G., Negreiros, T. O., and Bertoldo, C. (2018). "Moisture-related adjustment factor to obtain a reference ultrasonic velocity in structural lumber of plantation hardwood," *Wood Material Science and Engineering* 13(5), 254-261. DOI: 10.1080/17480272.2017.1313312

Guan, X., Zhao, M., and Wang, Z. (2013a). "Affection of propagation path of moisture content on the stress wave of wood," *Wood Processing Machinery* (2), 21-25. DOI: 10.13594/j.cnki.mcjgjx.2013.02.009

Guan, X., Zhao, M., and Wang, Z. (2013b). "Research progress in wood material testing based on stress wave technology," *Forestry Machinery & Woodworking Equipment* 41(2), 15-17. DOI: 10.3969/j.issn.2095-2953.2013.02.005

Li, X. (2015). *Key Technology Research on Material Performance and Damage Detection for Wooden Components of Ancient Chinese Building*, Ph.D. Dissertation, Beijing University of Technology, Beijing, China.

Li, X., Dai, J., Qian, W., and Chang, L. (2016). "Effect rule of different drill speeds on the wooden micro-drill resistance," *Journal of Beijing University of Technology* 42(7), 1066-1070. DOI: 10. 11936/bjutxb2015060080

Liao, C., Zhang, H., Li, D., Sun, Y., and Wang, X. (2012). "Influence of moisture content on the rapid detection index of wood properties," *Jiangsu Agricultural Sciences* 40(6), 280-282. DOI: 10.15889/j.issn.1002-1302.2012.06.020

Liu, H. (2014). *Theories and Factors of Wood Moisture Content Testing Based on Stress Wave Technology*, M.S. Thesis, Beijing Forestry University, Beijing, China.

Liu, H., and Gao, J. (2014). "Effects of moisture content and density on the stress wave velocity in wood," *Journal of Beijing Forestry University* 36(6), 154-158. DOI: 10.13332/j.cnki.jbfu.2014.06.002

Liu, Y., Wang, L., and Sun, M. (2014). "Study on the correlation between standing timber, log and board of Mongolian scotch pine in stress wave propagation velocity," *Forestry Machinery & Woodworking Equipment* (11), 42-47. DOI: 10.13279/j.cnki.fmwe.2014.0011

Llana, D. F., Íñiguez-González, G., Martínez, R. D., and Arriaga, F. (2018). "Influence of timber moisture content on wave time-of-flight and longitudinal natural frequency in coniferous species for different instruments," *Holzforschung* 72(5), 405–411. DOI: 10.1515/hf-2017-0113

Montero, M. J., De la Mata, J., Esteban, M., and Hermoso, E. (2015). "Influence of moisture content on the wave velocity to estimate the mechanical properties of large cross-section pieces for structural use of Scots pine from Spain," *Maderas. Ciencia y Tecnología* 17(2), 407–420. DOI: 10.4067/S0718-221X2015005000038

Moreno-Chan, J., Walker, J. C., and Raymond, C. A. (2011). "Effects of moisture content and temperature on acoustic velocity and dynamic MOE of radiata pine sapwood boards," *Wood Science and Technology* 45(4), 609–626. DOI: 10.1007/s00226-010-0350-6

Ni, Y., Tang, G., Zhang, Z., and Wang, C. (2019). "Study on the protection and repair methods of ancient wooden structures: Take the Diaodongge in Jingxian as an example," *Value Engineering* 38(23), 238-240. DOI: 10. 14018/j.cnki.cn13-1085/n.2019.23.100

Nocetti, M., Brunetti, M., and Bacher, M. (2015). "Effect of moisture content on the flexural properties and dynamic modulus of elasticity of dimension chestnut timber," *European Journal of Wood and Wood Products* 73(1), 51–60. DOI: 10.1007/s00107-014-0861-1

Peng, H., Jiang, J., Zhan, T., and Lu, J. (2016). "Influence of density and moisture content on ultrasound velocities along the longitudinal direction in wood," *Scientia Silvae Sinicae* 52(10), 117-124. DOI: 10.11707/j.1001-7488.20161015

Si, H., and Lu, Z. (2007). "Impact of growth characteristics of Larch wood on velocity propagating of the stress wave," *Wood Processing Machinery* 18(5), 14-16. DOI: 10.3969/j.issn.1001-036X.2007.05.005

Slavik, R., Cekon, M., and Stefanak, J. (2019). "A nondestructive indirect approach to long-term wood moisture monitoring based on electrical methods," *Materials* 12(15), Article Number 2373. DOI: 10.3390/ma12152373

Sun, Y. (2012). *Determining Wood Density and Mechanical Properties of Ancient Architectural Timbers with Micro-Drilling Resistance*, M.S. Thesis, Beijing Forestry University, Beijing, China.

The European Standard EN 384 (2004). "Structural timber-Determination of characteristic values of mechanical properties and density," London: BSI Publisher.

The Kingdom of wood. (2018). "Explain the types of moisture in wood," (http://www.yuzhuwood.com/news/details_40287d7363a6f39e0163a6fcf0d1000a.htm), Accessed 28 May 2018.

Timoshenko, S., and Doodier, J. (1970). *Theory of Elasticity*, 3rd Edition, McGraw-Hill, New York, NY, USA.

Wang, L., Gao, S., Wang, Y., and Xu, H. (2008). "Experiment on the propagation velocity of stress wave in frozen birch," *Journal of Northeast Forestry University* 36(11), 36-38. DOI: 10.13759/j.cnki.dlxb.2008.11.027

Wang, L., Wang, Y., Gao, S., Xu, H., and Yang, X. (2009). "Stress wave propagating velocity in *Larix olgensis* standing trees under a freezing condition," *Journal of Beijing Forestry University* 31(3), 96-99. DOI:10.13332/j.1000-1552.2009.03.023

Wang, X. (2008). "Effects of size and moisture on stress wave E-rating of structural lumber," in: *Proceedings of the 10th World Conference on Timber Engineering*, 2-5 June, Miyazaki, Japan, 9 p.

Wei, X., Sun, L., Sun, Q., Xu, S., Zhou, H., and Du, C. (2019). "Propagation velocity model of stress wave in longitudinal section of tree in different angular directions," *BioResources* 14(4), 8904-8922. DOI: 10.15376/biores.14.4.8904-8922

Xu, H. (2011). *Research on Stress Wave Propagation Velocity in Both Frozen and Unfrozen Wood*, Ph.D. Dissertation, Northeast Forestry University, Harbin, China.

Yang, X., and Wang, L. (2005). "Study on the propagation theories of stress wave in log," *Scientia Silvae Sinicae* 41(5), 132-138. DOI: 10.11707/j.1001-7488.20050524

Yu, B., Gao, S., Wang, L., Xie, W., and Hou, Y. (2014). "The study on the propagation law of ultrasonic wave in log," *Forest Engineering* 30(1), 92-99. DOI: 10.16270/j.cnki.slgc.2014.01.008

Zhang, H., Zhu, L., Sun, Y., and Wang, X. (2011). "Determining main mechanical properties of ancient architectural timber," *Journal of Beijing Forestry University*, 33(5), 126-129. DOI: 10.13332/j.1000-1522.2011.05.007

Zhu, L. (2012). *Determining the Mechanical Properties of Ancient Architectural Timber with Stress Waves*, M.S. Thesis, Beijing Forestry University, Beijing, China.

Zhu, L., Zhang, H., Sun, Y., and Yan, H. (2011). "Determination of mechanical properties of ancient architectural timber based on stress wave and micro-drilling resistance," *Journal of Northeast Forestry University* 39(10), 81-83. DOI: 10.13759/j.cnki.dlxb.2011.10.010

Article submitted: October 10, 2019; Peer review completed: December 1, 2019; Revised version received: January 13, 2020; Accepted: January 14, 2020; Published: January 17, 2020.
DOI: 10.15376/biores.15.1.1600-1616